

Identification of re-liquefaction potential based SPT and MASW data in Mpanau, Sigi after the earthquake 2018

Bayu Kusumajati^{1,2}, Ahmad Rifa'i^{1*}, and Istiarto Istiarto¹

¹Department of Civil and Environmental Engineering, Faculty of Engineering, Universitas Gadjah Mada, Yogyakarta Indonesia,

²Directorate General Water Resources, Ministry Public Work and Housing, Republic of Indonesia

Abstract. In September 2018, there was an earthquake followed by liquefaction which caused damage to thousands of houses and infrastructure in Central Sulawesi Province, Indonesia. Liquefaction in Central Sulawesi has the potential to recur, so identifying potential liquefaction in areas that have occurred is essential. The objective of this research is to compare the results of determining liquefaction potential based on geotechnical and geophysical data. Based on the peak ground acceleration earthquake value, it shows that the liquefaction potential obtained in Mpanau is resemblant. The simulation will be conducted using Settle3 software based on methods, then the values of Cyclic Resistance Ratio (CRR) and Cyclic Stress Ratio (CSR) will be compared based on existing Multi-Channel Analysis of Surface Waves (MASW) data. MASW needs to be considered in the way of potential identification because it is advantageous. This Research uses MASW data where liquefaction flow and damage do not occur in Mpanau area even though the potential is quite significant. The result of this research shows that at distinct points of the SPT, MASW and the 7.5 Mw earthquake resulted in potential liquefaction still present in several soil layers, especially in the Gumbasa canal. It is necessary to repair and countermeasure to prevent liquefaction from disrupting the irrigation system's performance.

1 Introduction

On 28 September 2018, Central Sulawesi Province, Indonesia, in particular Palu City and Sigi Regency experienced earthquakes shocks. The earthquakes were destructive, and the disaster, which was followed by liquefaction, also claimed many thousands of lives. Liquefaction events are apparently not a new thing in the life of the Kaili Tribe (an indigenous tribe in Palu City) because they have their own term, "Nalodo", to refer to subsidence events sucked in by mud, so they avoid the "Nalodo" risk areas [1].

Liquefaction events have a great potential to recur, so areas that have the liquefaction potential or have experienced liquefaction require further investigation so that structural and non-structural policies can be carried out to avoid damage and victims in the future. The most common occurrence in the study locations is sand boiling in several areas, indicating the occurrence of liquefaction events.

This research aims to compare the results of determining liquefaction potential based on geotechnical (SPT data) and geophysical data (Vs data).

2 Method

2.1 Location

The research is located in Gumbasa irrigation main canal (8,180 Ha), which during the 2018 earthquake was damaged not only because of the earthquake that occurred but several points were also damaged due to liquefaction. This research is devoted to the Gumbasa main canal in Mpanau Village or the BGKn52-57 irrigation channel (Gumbasa Rightside Building No 52-57). The study location map is in Fig. 1.

2.2 Data

This Research uses ground investigation data for the Gumbasa Irrigation Area by Ministry of Public Work and Housing financed by the Asian Development Bank (ADB), which will be carried out along the Gumbasa irrigation canal in 2021. Liquefaction potential will be measured using Standard Penetration Test (SPT) and MASW (Multi-channel Analysis of Surface Waves) data. Besides that, MASW data is also the basis for determining the class of rock sites at the study site.

Standard Penetration Test is carried out at each drill point at an interval of 1.5 to 3 meters depth. Standard Penetration Test (SPT) is carried out on soil or weathered rock layers to determine the consistency of fine-grained soil and coarse-grained soil density

*Corresponding author: ahmad.rifai@ugm.ac.id

following [3]. SPT is held together with drilling to know both the dynamic resistance of the soil and taking the sample that is disturbed by the collision technique. The SPT test consists of hitting a thick wall split tube into the ground and measuring the number of blows to insert a divided tube as deep as 45 cm vertically. In this drop load system, a hammer weighing 63.5 kg is repeatedly

dropped with a falling height of 0.76 m. The test is carried out in three stages, namely 3 x 15cm thick in succession. The first stage is recorded as a stand seat, while the number of strokes to enter the second and third stages is added to obtain the value of N strokes or SPT resistance.

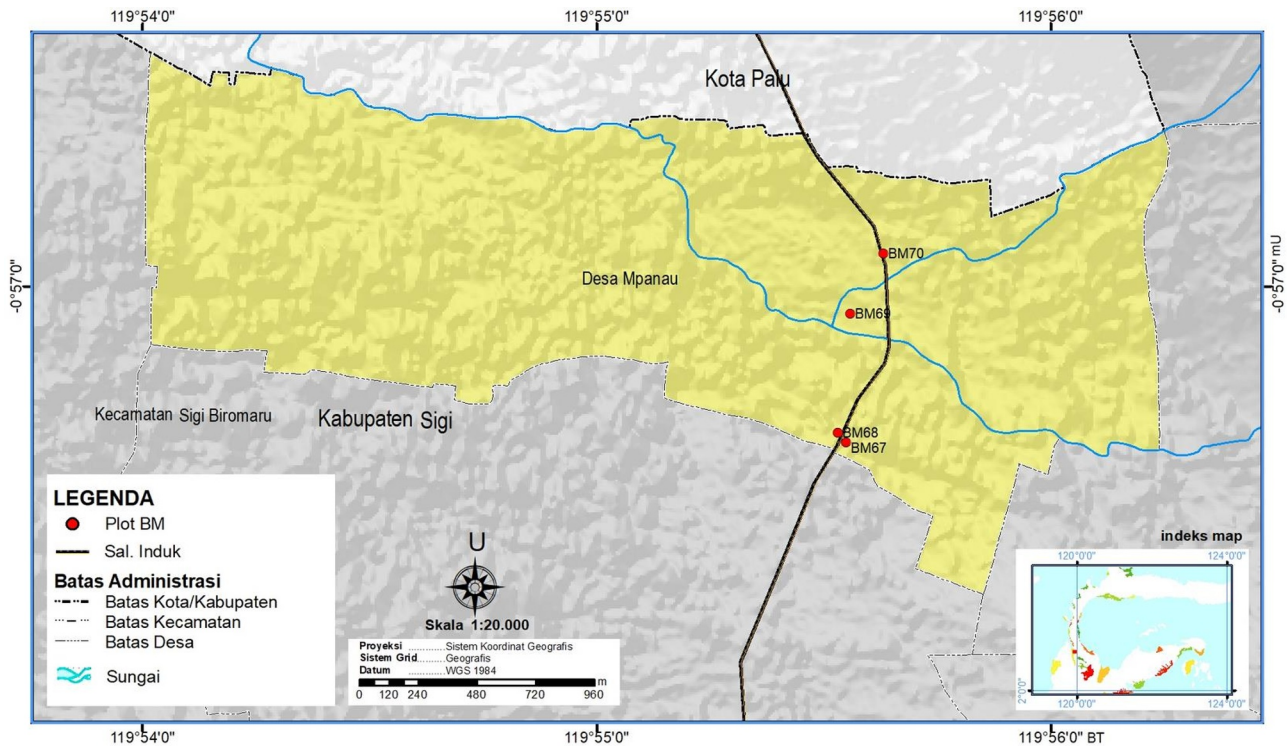


Fig. 1. Study location in Mpanau (BIG with modified) [2].

In general, liquefaction occurs in soils with an SPT N value of <25 [22], assuming that soft to moderate clay will partially liquefy under certain conditions. Based on

the results of collecting SPT data, Stratigraphy was then formed, as shown in Fig. 2.

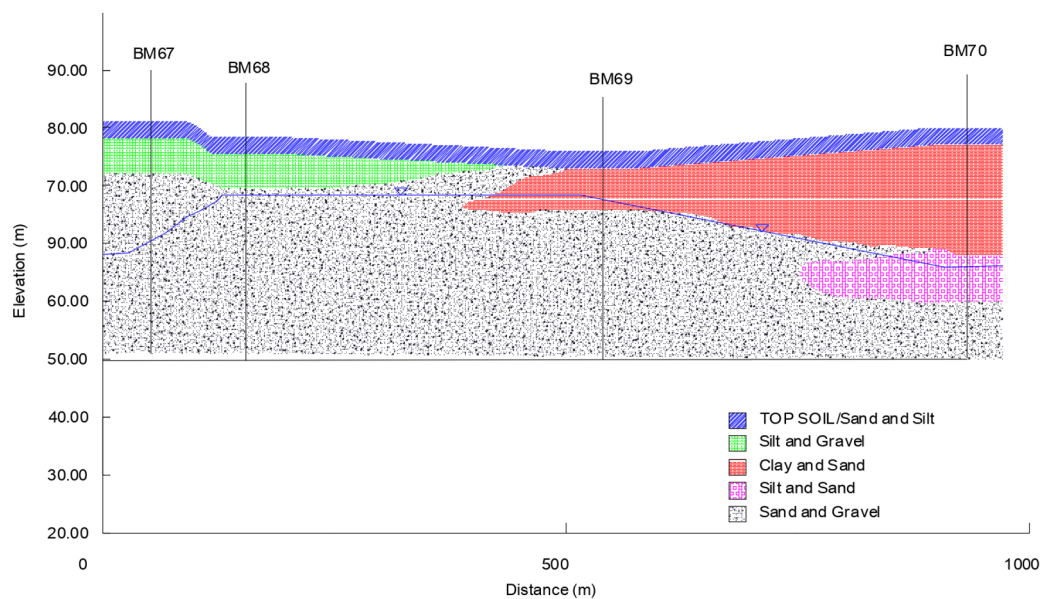


Fig. 2. Stratigraphy based on four SPT test points.

Determination of liquefaction potential using two boreholes of SPT with nomenclature BM68 at groundwater level -5m and BM69 at -3.82m. Liquefaction is very probable in areas where groundwater is mainly located within 10 m of the ground surface; few examples of liquefaction have occurred in areas with groundwater deeper than 20 m [5-6]. Compacted soils, including well-compacted embankments, have a low susceptibility to liquefaction [7].

The use of Vs data has several advantages, namely the process of collecting data in the field can be carried out on soils that are difficult to sample, such as gravel soil. Vs data is required in response to soil site class. The weakness of this method is that it requires some secondary data to complete the data so that it can analyze soil that has the potential for liquefaction, namely data on soil type, soil density and depth of the groundwater table.

MASW at the study site was carried out at 2 points, each adjacent to BM68 and BM 69. Data acquisition

uses 24 geophones that are installed in a straight line, and the distance between the geophones is 5 meters, while the offset for the SP (shoot point) is 5 meters; the results will get several types of waves such as direct waves, refracted waves, reflection waves, and ground. Roll. The basic concept of the MASW survey in measuring V_{s30} by using the principle of wave propagation Rayleigh or Ground roll surface, which is dispersive.

Apart from various data acquisition parameters, topographical conditions are known to have an effect on the quality of the recorded surface wave data and, therefore, the quality of the resulting dispersion curves. For optimum results, the receivers should be placed on relatively flat terrain. Thus, during data acquisition, several MASW spread designs were moved from the original plan. The location of the test line is shown in Fig. 3.

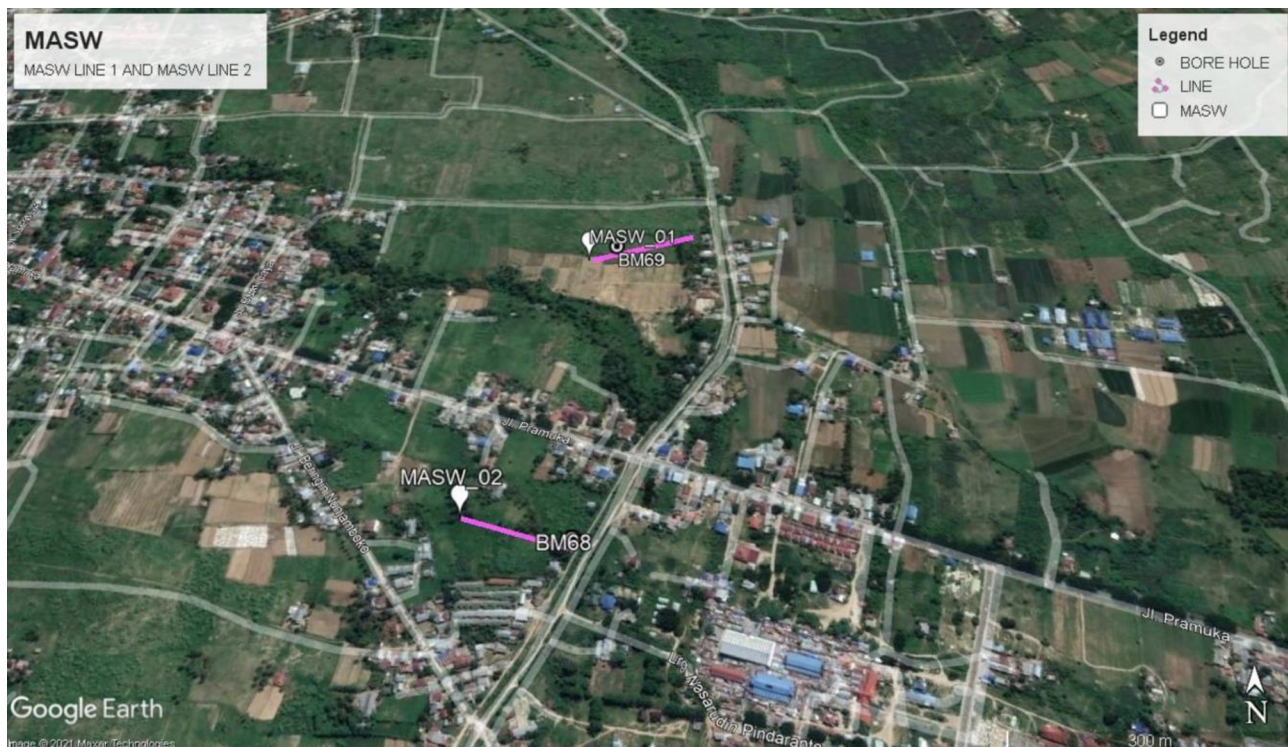


Fig. 3. Study location in Mpanau (Google Earth modified).

2.3 Methods

To find out the potential for liquefaction based on N-SPT data is to get the value of the safety factor from the comparison of the CRR (Cyclic Resistance Ratio) value with CSR (Cyclic Stress Ratio). The factor of safety used should not be less than one because if it is less than one, then the soil will experience liquefaction. The Magnitude Scaling Factor (MSF) is used to determine CSR and/or CRR using the usual M value (conventionally taken as $M=7.5$) because CRR depends on the amount of cyclic load, which is correlated with the magnitude value (M) [8].

Furthermore, the value $(N1)_{60}$ is used to calculate the Cyclic Stress Ratio (CSR), Cyclic Resistance Ratio (CRR) and Factor of safety (FS) using two methods. The method [9] is an analysis of liquefaction potential based on a comparison of CSR and CRR, with CSR whose depth reduction factor r_d is determined based on the depth range. The CRR value is selected from the SPT value, which is corrected based on the FC value. Calculation of CSR and CRR based on SPT data uses Settle3 Rockscience software which will produce graphs based on the method. The methods presented in this simulation are based on Idriss and Boulanger [8] and Cetin [10].

According to ASTM, each SPT test equipment used must be calibrated for its energy efficiency level by using gauges, strain gauges and accelerometers to obtain more accurate energy efficiency standards. If the efficiency measured (Ef) obtained from the measured style calibration must be corrected for the efficiency of t, the value of N is 60% and is expressed in the formula Equation 1 [11].

$$N_{60} = \frac{E_f}{60} NM \quad (1)$$

where N60 is efficiency 60%; Measured efficiency Ef and N SPT test values.

Seed and Idriss [12] stated that in obtaining the cyclic pressure induced by the earthquake, which affects the liquefaction potential is 65% of the peak cyclic pressure. This is what is called the Cyclic Stress Ratio (CSR), which is formulated as follows Equations 2-3.

$$CRR_{7,5} = 0,022 \left(\frac{V_{s1}}{100} \right)^2 + 2,8 \left(\frac{1}{V_{s1}^* - V_{s1}} - \frac{1}{V_{s1}^*} \right) \quad (2)$$

$$CSR = 0,65 \frac{\tau_{max}}{\sigma'_{vc}} = 0,65 \frac{\sigma_{vc}}{\sigma'_{vc}} \frac{a_{max}}{g} r_d \quad (3)$$

PGAm calculations use the Kanno method, and site class determination is based on SNI 1726:2019. This equation is used to estimate PGA in shallow areas, and in calculating the PGA value in Equations 4-5 [13].

$$\log pre = a_1 M_w + b_1 X - \log(X + d_1 10^{0.5 M_w}) + c_1 \text{ for } D \leq 30 \text{ km} \quad (4)$$

$$\log pre = a_2 M_w + b_1 X - \log(X) + c_2 \text{ for } D \geq 30 \text{ km} \quad (5)$$

That curve Fig. 4 can use to determine potential liquefaction for the average fine content range between 6% and 34%, the average fine content for BM68 is 13.58% and 6.76%.

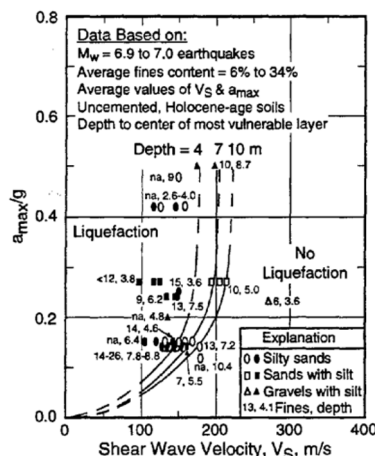


Fig. 4. Comparison vs and amax [16].

The Multi-channel Analysis of Surface Wave (MASW) method produces data that is on the surface by analyzing Rayleigh waves by utilizing the ground roll dispersion properties using shear wave velocity data (Shearer, 2009). From the resulting data Vs profile, we can determine the class site with an average Vs at a depth of 30 m (Vs30), the thickness of the soil layer and bedrock layer for analysis of liquefaction potential [14]. Vs data is also often used for classifying rocks as a result of earthquakes, so it is often used to test earthquake-resistant buildings and mitigate disaster [15].

Andrus and Stokoe developed standard criteria for liquefaction resistance based on 26 earthquake events and shear wave velocity sampling at 70 points, shown in Fig. 4 the curve displays CSR with Vs with an earthquake Mw = 7.5 then separates the parts that have the potential to experience liquefaction or are safe from it [16].

The curve connecting PGAm and Vs to determine the liquefaction zone is presented in Fig. 4.

MASW is a near-surface method that is often used because it can provide information on shear wave velocity (Vs) to investigate near-surface structures in an effective, inexpensive, efficient, and easy to process. Usually, a source frequency of 3-30 Hz is used for data retrieval, and a multi-channel recorder (geophone) is arranged lengthwise. The writer used can be as many as 12 or 24, with a distance between recorders is the same [17].

The MASW in the Fig. 5 method is prevalent in identifying earthquake shock prone zones and is classified by site class, which refers to the value of shear wave velocity (Vs30) by Eurocode 8, MASW can be carried out in 3 stages, namely:

1. MASW data acquisition,
2. Extraction of the Dispersion Curve,
3. Inversion of the Dispersion Curve

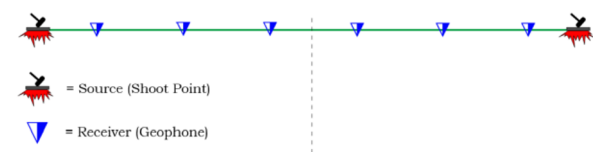


Fig. 5. MASW acquisition design.

The results of the 1D model of shear wave velocity are then interpreted using Vs30. Vs30 is the shear wave velocity up to a depth of 30 meters from the ground surface. Value Vs30 used in determining earthquake-resistant building standards and is also used for deciding rock classification based on the strength of vibrations from earthquakes due to local effects. This is because the layers of rock up to a depth of 30 meters determine the the magnitude of the earthquake waves.

3 Result

3.1 Settle3D

Settle3D is a software developed by Rocscience that offers various methods of calculating the factor of safety

related to liquefaction resistance, liquefaction probability and the input parameters required for the calculation [18]. The analysis used in this application is based on Standard Penetration Test (SPT), Cone Penetration Test (CPT), and/or Shear Wave Velocity (VST) data. Calculations based on SPT data, for liquefaction trigger analysis can be carried out using the Pre-defined Triggering Methods or Customized Triggering Methods [19]. The graphical results for the SPT for each layer along with the corrected SPT values that have been simulated using Settle3 are shown in the Fig. 6 . This tool generates the liquefaction probability as factor of safety [20]

In general, the condition of the soil is in the form of loose sand, which has the correlation with the SPT value.

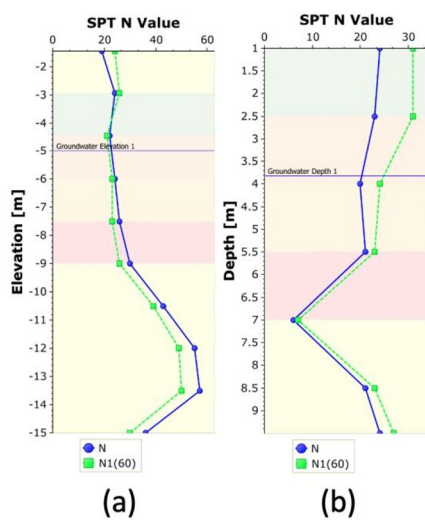


Fig. 6. (a) SPT value BM68; (b) SPT value BM69.

3.2 Peak ground acceleration

Then based on Then the Peak Ground Acceleration (PGA) calculations using the Cipta Karya standard [21] that compare with Kanno Method (2006), the PGA in the Mpanau study area is 0.43 g

PGA_M values can also be used to analyze liquefaction potential in an area [22]. Ministry of Public Work and Housing Republic of Indonesia built a website to calculate the two acceleration values mentioned above. The latest version developed is *rsaciptakarya.pu.go.id* which was built in 2021 [23]. the web view in Fig. 7 shows a PGA value of 0.33.

Based on SNI 1726:2019 the PGA (Table 1) value is multiplied by the site class coefficient, that is, both locations are SD site classes multiplied by 1.2 and the result is 0.58. RSA Cipta Karya produced a PGA of 0.61 and the Kanno Method of 0.58, so a value of 0.6 was chosen as the basis for the following calculation.

Then calculated using Settle3 so that the CRR and CSR values at each point are still presented in the Fig. 8. Calculation CSR and CRR (a)BM68 (b)BM69.

3.3 Shear wave

A recording frequency (fs) of 1000 Hz is used in out MASW surveys, which is corresponds to a sampling interval (dt) of 1 ms. The total recording time is 2 seconds because we consider the spread length of the receiver (24 meters and 48 meters for VS₁₀ and VS₃₀, respectively), an impulsive seismic source (a sledgehammer), and very low shear wave velocities are expected. The maximum investigation depth (Zmax) is determined by the longest surface wavelength that is obtained during data acquisition.

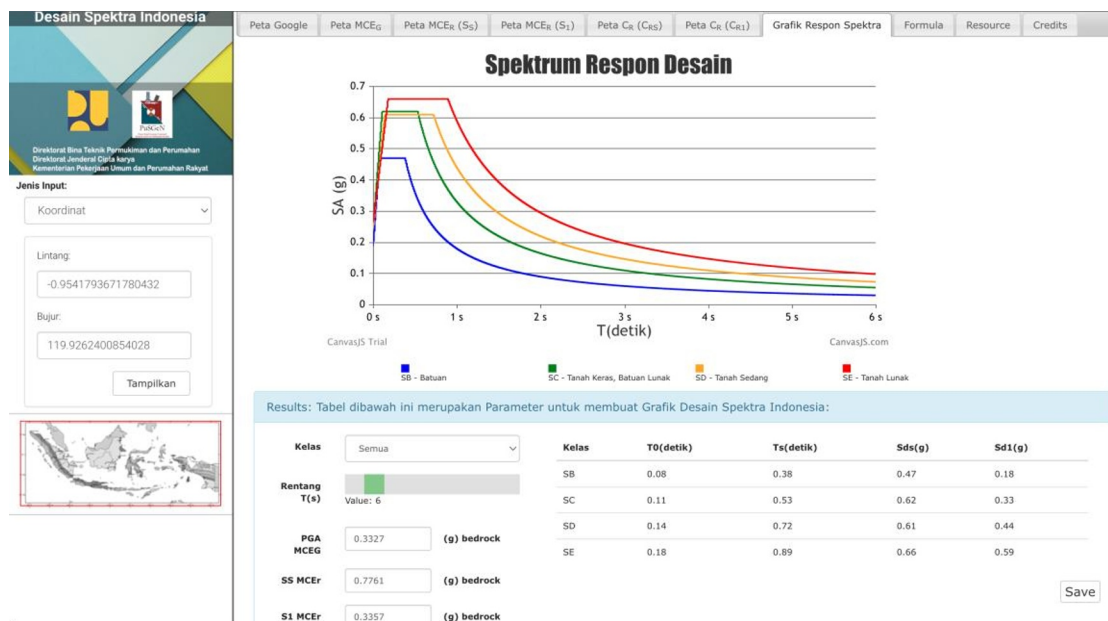


Fig. 7. PGA calculation [21].

Table 1. PGA calculation based kanno (2006) [13].

Loc	Epicerter (km)	Hipocenter (km)	Log PGA (cm/sec ²)	PGA (g)
BM68	86.95	87.52	2.4851	0.3115
BM69	86.48	87.05	2.4883	0.3138

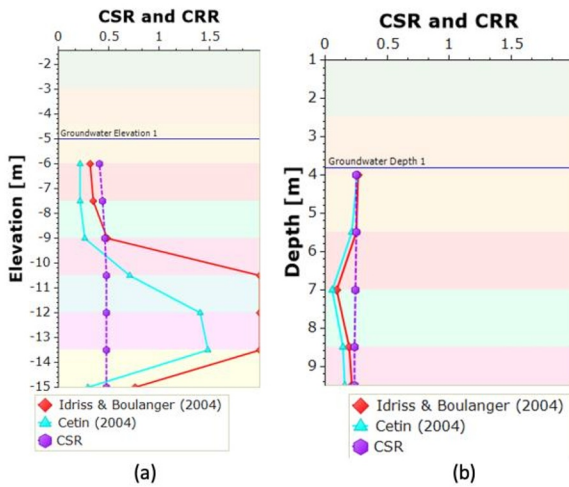


Fig. 8. Calculation CSR and CRR (a)BM68 (b)BM69.

Fig. 9 show profile beneath Line 1 (L01) and the corresponding Borehole (BM69) which is located 40

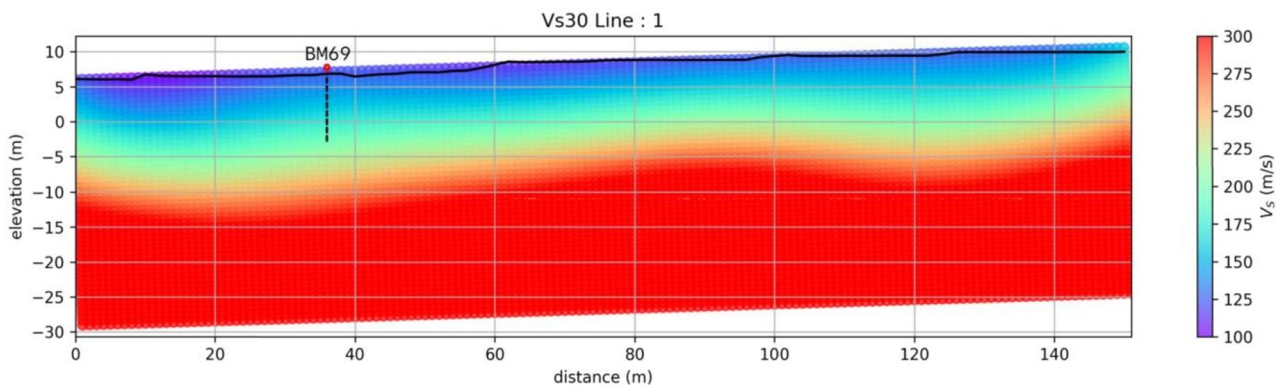


Fig. 9. 2D shear wave velocity from VS30 Line 01.

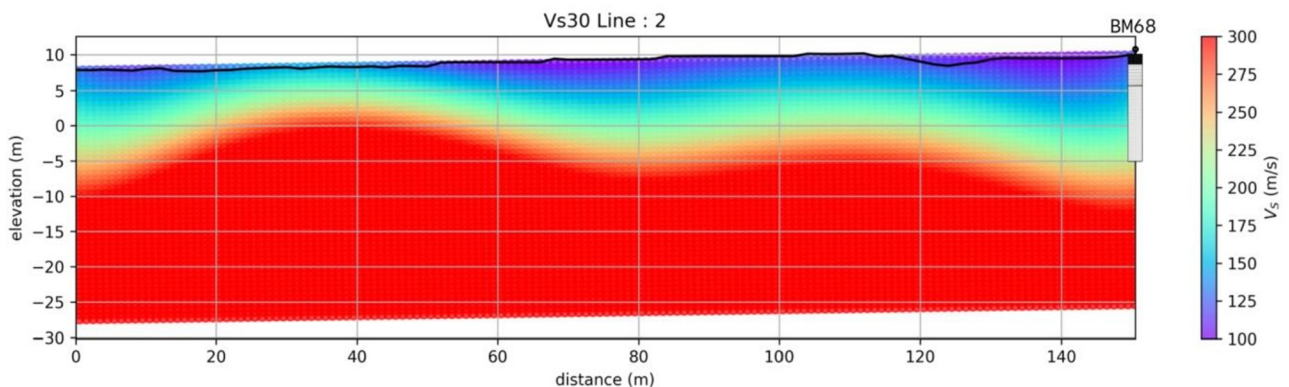


Fig. 10. 2D Shear Wave Velocity from VS30 Line 02 [5].

meters away, perpendicular to the survey line at 36 m. and Fig. 10 2D shear wave velocity from VS30 profile beneath Line 2 (L02) and the corresponding Borehole (BM68) which is located in line with the survey line at 150 m.

The shear wave velocity match well with the borehole stratigraphy data. In general, the shear wave velocity at the survey field ranges from 100 m/s to 300 m/s, which indicates that the subsurface conditions range from soft-soil to medium-soil (Table 2).

Which are Line 1, show that the shear wave velocities in the subsurface profile for the lines is less than 175m/s before depth of 7 meter which according to USGS [25] and SNI 1726:2019 [24] classification is soft-soil. The shear wave velocity profile then gradually increases to the west, and the velocity less than 175m/s visible less than a depth of 5 meters. Low shear wave velocity variations seen in which are Line 2.

From the Averaged of shear wave velocity value, we can conclude that Classification of medium-soil (SD) for VS₁₀ can be found in Line 1, and the Classification of soft-soil (SE) for VS₁₀ can be found in Line 2. However, to determine the site class VS₃₀ is used so that Line 1 and Line 2 are SD site classes shown in Fig. 11.

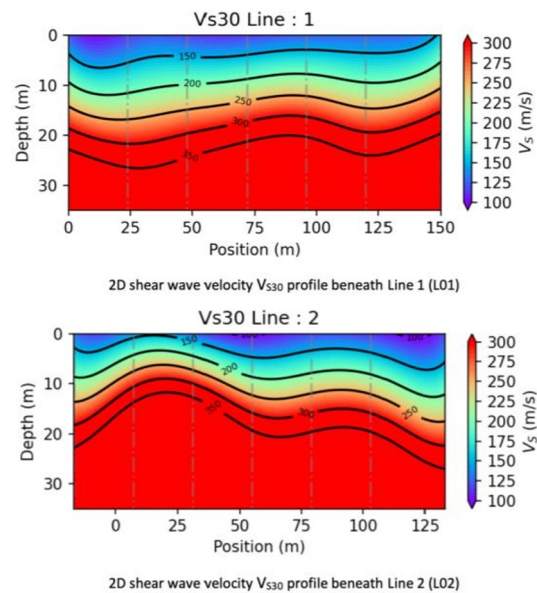


Fig. 11. MASW value clasification [5].

Table 2. Classification of rock according to the speed of wave progation (V_s) [24]

Soil Type	General Description	V_s (m/s)
SA	Hard Rock	$V_s \geq 1500$
SB	Rock	$750 < V_s \leq 1500$
SC	Soft Rock	$350 < V_s \leq 750$
SD	Medium Soil	$175 < V_s \leq 350$
SE	Soft Soil	$V_s < 175$
SF	Special Soil	Require special evaluation

4 Discussion

The CRR and CSR calculated using the Settle3 application are then continued with calculations to obtain the safety factor (FS) and determine the probability of liquefaction in each soil layer. The number is likely to appear in each soil layer. In this case, probabilities are shown using the Cetin [10] and Youd and Noble [9] methods, while for FS or other methods, namely Idriss and Boulanger, [26] it can also be simulated. The value at each point is displayed in the graphic Fig. 12.

Based on the calculation graph in Fig. 12, at point BM68, the liquefaction potential still exists at an elevation of -4 to -9 but not too big. Whereas in BM69, all layers of soil down to a depth of -10 m have the potential for liquefaction in all calculation methods, but the probability according to [10] is small in the top soil layer.

Comparison between the results of SPT and V_s (Fig. 13) can be helpful in complete data on soil layers that have not been tested with SPT because the depth does not reach 30 m. by reading the curve so that it can be seen that the layers intersect between the two tests.

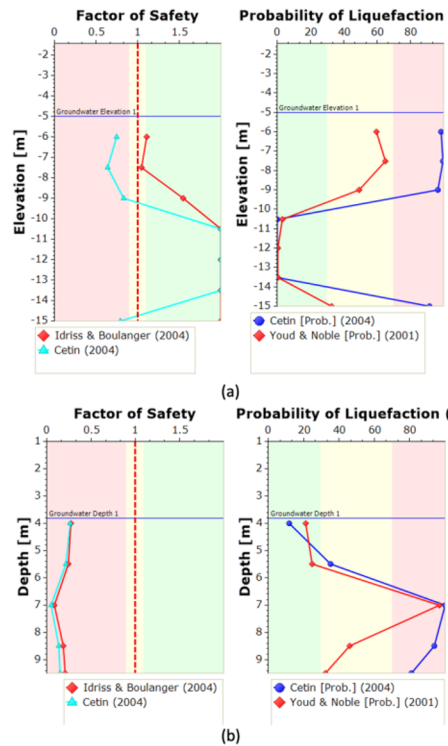


Fig. 12. Factor safety and probability of liquefaction at each point SPT (a)BM68; (b)BM69.

Comparison between the results of SPT and Vs (Fig. 13) can be helpful in complete data on soil layers that have not been tested with SPT because the depth does not reach 30 m. by reading the curve so that it can be seen that the layers intersect between the two tests.

The image below compares the Vs and PGA values in each soil layer. The value of Vs included in the curve is only for layers in water-saturated conditions as the existing theory states that liquefaction only occurs in water-saturated layers. Then points are also distinguished between points that intersect with the SPT test and do not overlap.

Table 3 and Fig. 13 describe the potential for liquefaction in each layer of soil. The depth follows the SPT test reading, so the Vs value is used based on that depth. The determination of liquefaction potential based on the SPT test can be seen in the Settle3 output graph, while the Vs value is based on the boundary on the curve in Fig. 14 and Fig. 15.

In line 1 all layers have the same liquefaction potential, but in line 2 there are some differences in layers with liquefaction potential.

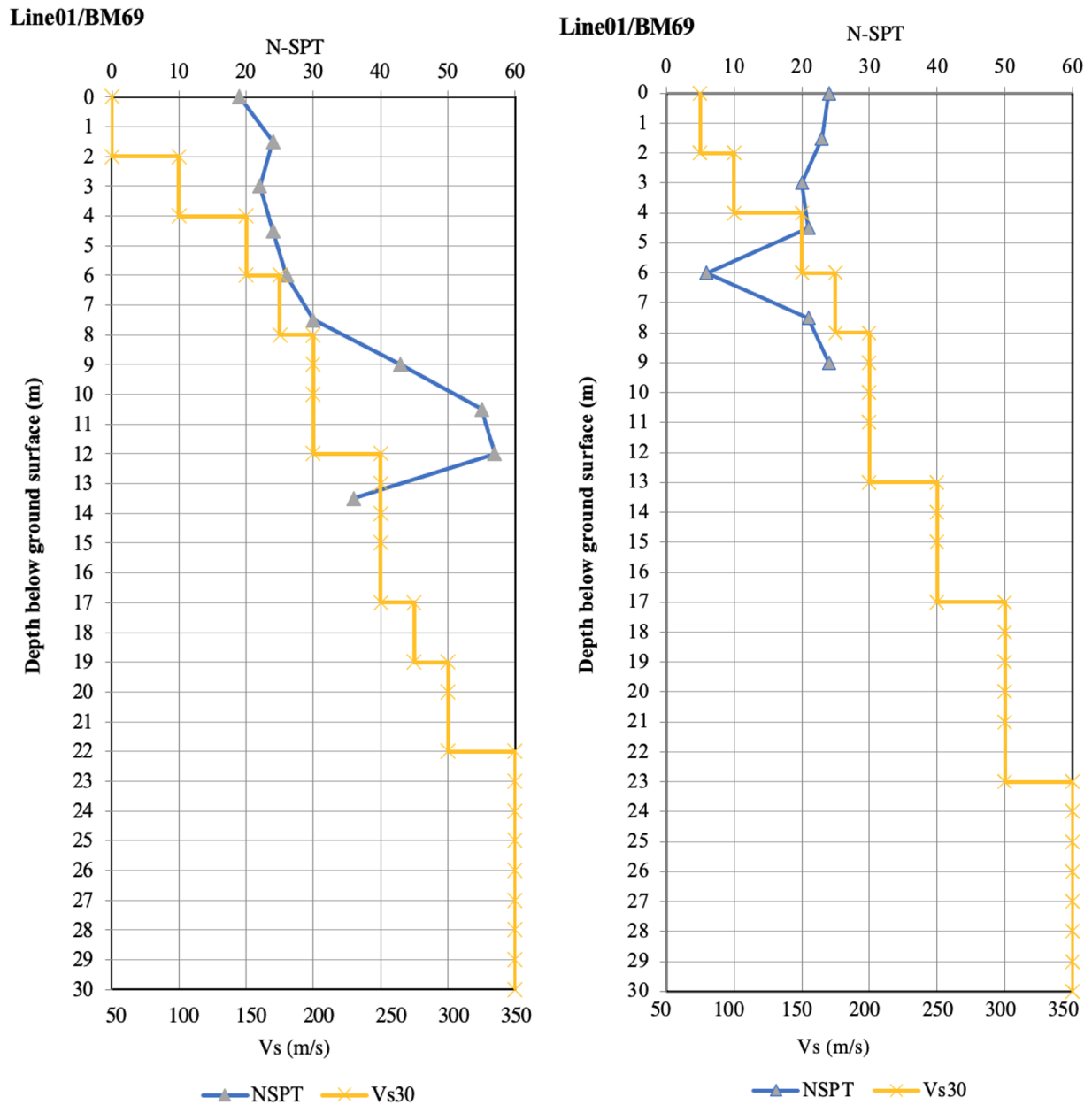


Fig. 13. Comparison graph vs and SPT.

Table 3. Result per layer Line 1/BM69.

Depth (m)	Vs	SPT
4	Liq	Liq
5.5	Liq	Liq
7	Liq	Liq
8.5	Liq	Liq
9.5	Liq	Liq
10	Liq	Liq
15	No	N/A
20	No	N/A
25	No	N/A
30	No	N/A

geophysical approach can be done, but for geophysical calculations, it requires fine content testing.

Table 4. Result per layer Line 2/BM68.

Depth (m)	Vs	SPT
5	Liq	No
6	Liq	Liq
7.5	Liq	Liq
9	Liq	Liq
10.5	Liq	No
12	No	No
13.5	No	Liq
15	No	Liq
20	No	N/A
25	No	N/A
30	No	N/A

5 Conclusion

Determining the liquefaction potential based on SPT data as a geotechnical approach and MASW as a

At a PGA value similar to the earthquake that occurred in 2018, the Mpanau location has the potential for repeated liquefaction in several layers. However, the MASW results show that the potential for liquefaction is greater in the investigated soil layers.

The ground water level at the research location is 3.82 m and 5 m respectively so that both are only modeled on saturated soil conditions. As a result, for the first point or BM 68 the two approaches are the same, showing that layers at a depth of 4 m to 10 meters have

the potential for liquefaction. This is different from the second point or BM69 according to Vs, the depth point of 5 m-10 has the potential to experience liquefaction, but according to SPT data calculations, the depth of the layer that is experiencing liquefaction is 6 m -10.5 m and 13.5 m - 15 m.

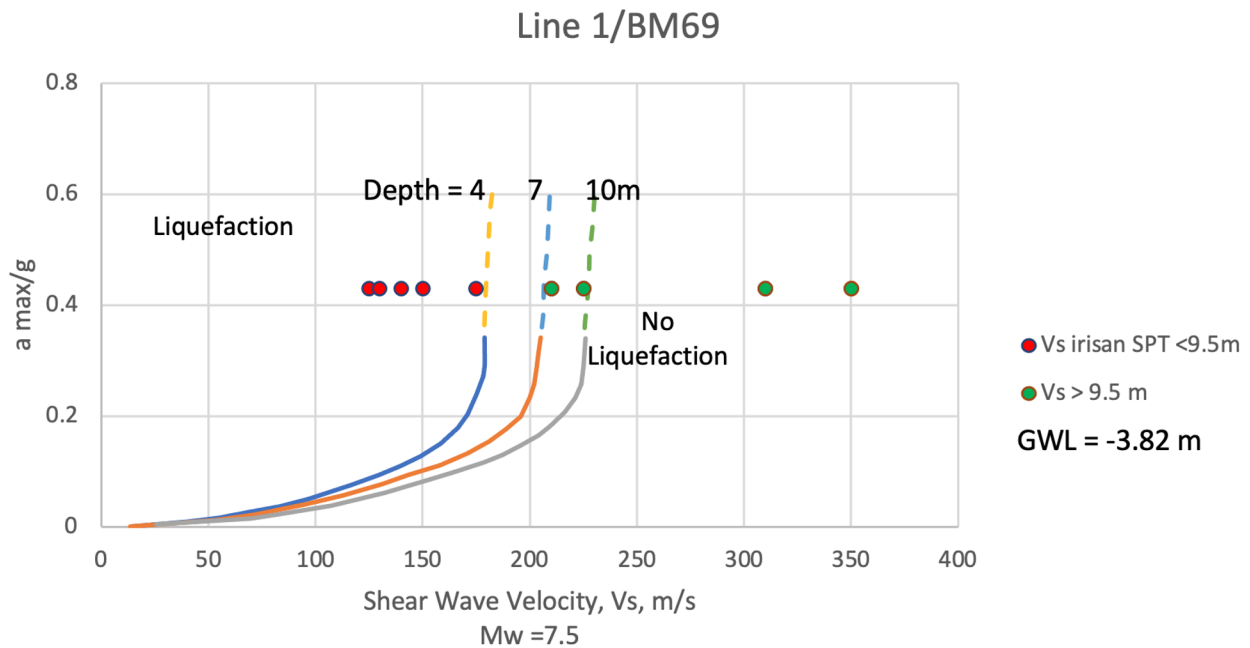


Fig. 14. Plot vs and PGA on Line 1.

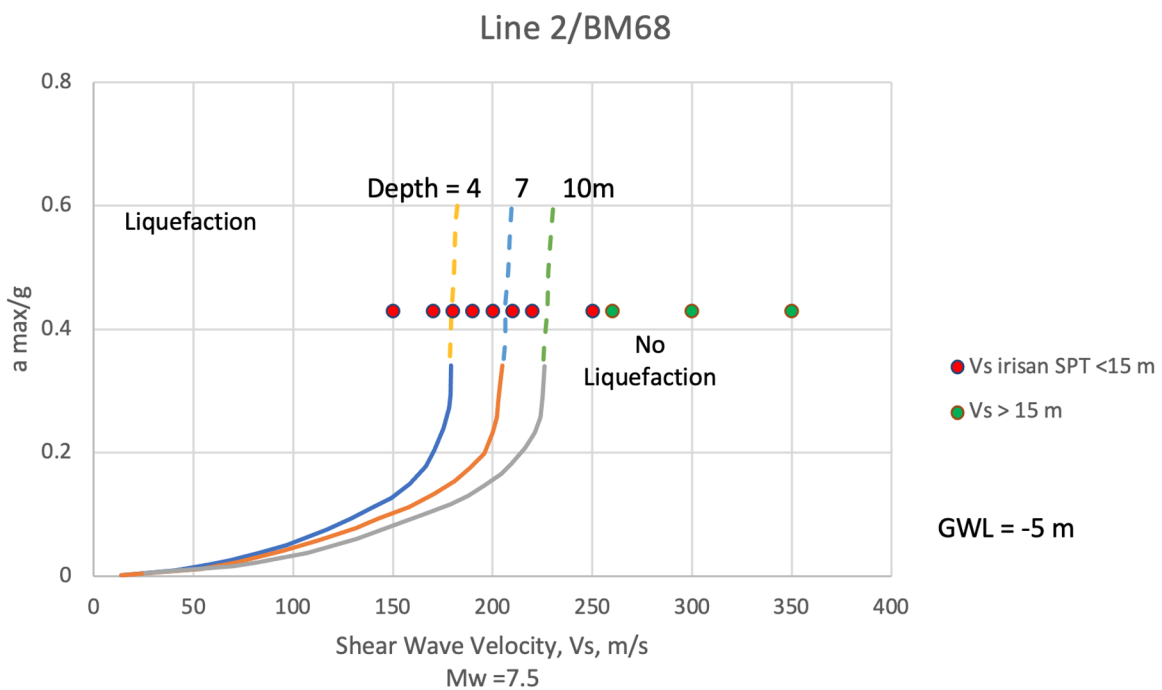


Fig. 15. Plot vs and PGA on Line 2.

SPT and MASW data can be used in determining liquefaction potential. The accuracy of using SPT data is better because it describes each layer of soil based on the original conditions. However, MASW data is cheaper and easier to sample.

Although this research uses methods that can be applied in engineering, several other methods to calculate liquefaction potential can be used by implementing geotechnical and geophysical approaches.

The authors would like to express their gratitude for the support given by Ministry of Public Work and Housing, Republic of Indonesia.

References

1. A. Tohari, Study of the Central Sulawesi Palu earthquake 28 September 2018 (M7,4) (Housing and Settlements Research and Development Center, 2019)
2. Geospatial Information Agency Republic of Indonesia (accessed 3 December 2022, 2017) <https://tanahair.indonesia.go.id/portal-web>
3. National Standardization Agency, Field penetration test method with SPT (SNI 4153:2008)
4. L. Zeevaert, Foundation engineering for difficult subsoil conditions (Van Nostrand Reinhold Company, 1972)
5. Ministry Public Work and Housing and Japan International Cooperation Agency, Boring survey for basic response for Central Sulawesi earthquake (2019)
6. T.L. Youd, J.C. Tinsley, D.M. Perkins, E.J. King, R.F. Preston, *Liquefaction potential map of San Fernando Valley, California*, in Int. Conf. on Microzonation for Safer Construction, San Francisco (1978)
7. V. Bertero, Greene, T.L. Youd, M. Power, Earthquake basics brief No. 1 (Earthquake Engineering Research Institute, 1994)
8. I.M. Idriss, R.W. Boulanger, Soil liquefaction during earthquake (Earthquake Engineering Research Institute, 2008)
9. T.L. Youd, I.M. Idriss, R.D. Andrus, I. Arango, G. Castro, J.T. Christian, R. Dobry, W.D.L. Finn, L.F. Harder, M.E. Hynes, K. Ishihara, J.P. Koester, S.S.C. Liao, W.F. Marcuson, G.R. Martin, J.K. Mitchell, Y. Moriwaki, M.S. Power, P.K. Robertson, R.B. Seed, K.H. Stokoe, Journal of Geotechnical and Geoenvironmental Engineering **127**(10), 817-833 (2001) [https://doi.org/10.1061/\(ASCE\)1090-0241\(2001\)127:10\(817\)](https://doi.org/10.1061/(ASCE)1090-0241(2001)127:10(817))
10. K.O. Cetin, R.B. Seed, A.D. Kiureghian, K. Tokimatsu, L.F. Harder, R.E. Kayen, R.E.S. Moss, Journal of Geotechnical and Geoenvironmental Engineering **130**, 1314 (2004)
11. H.C. Hardiyatmo, Foundation engineering I, 1st Ed. (PT Gramedia Pustaka Utama, 1996)
12. H.B. Seed, I.M. Idriss, Journal of the Soil Mechanics and Foundations Division **97**(9), 1249 (1971) <https://doi.org/10.1061/JSFEAQ.0001662>
13. T. Kanno, A. Narita, N. Morikawa, H. Fujiwara, Y. Fukushima, Bulletin of the Seismological Society of America **96**(3), 879-897 (2006) <https://doi.org/10.1785/0120050138>
14. R. Villaverde, Fundamental concepts of earthquake engineering (CRC Press-Taylor and Francis Group, 2009)
15. H. Sucuoğlu, S. Akkar, Basic earthquake engineering: From seismology to analysis and design (Springer Cham, 2014) <https://doi.org/10.1007/978-3-319-01026-7>
16. R.D. Andrus, K.H. Stokoe II, Journal of Geotechnical and Geoenvironmental Engineering **126**(11), 1015-1025 (2000) [https://doi.org/10.1061/\(ASCE\)1090-0241\(2000\)126:11\(1015\)](https://doi.org/10.1061/(ASCE)1090-0241(2000)126:11(1015))
17. C.B. Park, R.D. Miller, J. Xia, J. Ivanov, The Leading Edge **26**(1) 1015-1025 (2007) <https://doi.org/10.1190/1.2431832>
18. Rocscience Inc, Settle3D liquefaction theory manual (2023)
19. H. Muhanifah, Undergraduate Thesis (Universitas Gadjah Mada, 2022)
20. A. Maulana, R. Ahmad, F. Fikri, E3S Web Conf. **156**, 02003 (2020) <https://doi.org/10.1051/e3sconf/202015602003>
21. Ministry Public Works and Housing, Directorate general human settlement (accessed 10 December 2022, 2021) <https://rsa.ciptakarya.pu.go.id/2021/>
22. A. Jalil, I. Satyarno, T.F. Fathani, W. Wilopo, International Journal of GEOMATE **18**(65), 147-155 (2020) <https://doi.org/10.21660/2020.65.94557>
23. W. Partono, M. Irsyam, R. Nazir, M. Asrurifak, F. Kistiani, U.C. Sari, Media Komunikasi Teknik Sipil **27**(2), 203-212 (2021) <https://doi.org/10.14710/mkts.v27i2.40714>
24. National Standardization Agency, Seismic Resistant Design Guidelines for Building and Non-building Structures (SNI 1726:2019)
25. USGS, The United States Geological Survey 2023 (2023)
26. I.M. Idriss, R.W. Boulanger, Soil Dynamics and Earthquake Engineering **26**(115), 203-212 (2004)